Afyon Kocatepe Üniversitesi Fen ve Mühendislik Bilimleri Dergisi
Afyon Kocatepe University – Journal of Science and Engineering
https://dergipark.org.tr/tr/pub/akufemubid

Araştırma Makalesi / Research Article
e-ISSN: 2149-3367
DOI: https://doi.org/10.35414/akufemubid.1560061
AKÜ FEMÜBİD **25** (2025) 041203 (738-756)
AKU J. Sci. Eng. **25** (2025) 041203 (738-756)

The Composite Microbeads of Alginate, Carrageenan, Gelatin, and Poly-(Lactic-co-Glycolic Acid): Swelling, Cefaclor Loading and Release

Makale Bilgisi / Article Info
Alındı/Received: 04.10.2024
Kabul/Accepted: 03.02.2025
Yayımlandı/Published: 04.08.2025

Aljinat, Karragenan, Jelatin ve Poli-(Laktik-ko-Glikolik Asit) Kompozit Mikroboncukları: Şişme, Sefaklor Yükleme ve Salınımı

Buse SEMERCİ ARIKAN[1*], Demet BAYBAŞ[2]

[1] *Malatya Turgut Özal Üniversitesi, Tıp Fakültesi, Tıbbi Biyokimya Ana Bilim Dalı, Malatya, Türkiye*
[2] *Sivas Cumhuriyet Üniversitesi, Fen Fakültesi, Biyokimya Bölümü, Sivas, Türkiye*

Abstract

The controlled release of drugs under desired conditions after attachment to a support material has been of interest to many researchers for some time. The aim of this study was to synthesize composite microbeads consisting of a combination of two (AC, AG, AP), three (ACG, ACP, AGP) or four (ACGP) of the components alginate (A), carrageenan (C), gelatin (G) and/or poly (lactic-co-glycolic acid) (P) and to investigate the usability of the beads for drug delivery. The antibiotic cefaclor (Cef) was chosen as the model drug. Fourier Transform Infrared (FTIR) spectra of drug and drug-free composite microspheres synthesized under different conditions were compared. The effects of synthesis conditions such as component amounts, and cross-linking ion amounts on swelling, retention efficiency and release kinetics of the materials were investigated. Alginate-containing microbeads, which have the highest swelling capacity of 157-981% (AG-A), can be described as hydrogel materials. The addition of PLGA to alginate beads reduces the swelling capacity, whereas the addition of PLGA to composite beads containing other components increases the swelling percentage. As the amount of PLGA added to the ACP beads increases, swelling decreases. The maximum entrapment efficiency of cefaclor in micro-composites varies between 36-93% (A-ACP). All release experiments were performed in simulated gastric fluid at body temperature without enzymes, with fresh solutions under shaking conditions. In general, no burst effect was observed in the release of cefaclor from composite beads. The selected data are fitted to Korsmeyer Peppas, Higuchi drug release models, zero and first-order release kinetics.

Keywords *Cefaclor-release; Alginate; Carrageenan; Gelatin; Poly(lactic-co-glycolic acid)*

Öz

İlaçların bir destek malzemeye tutturulduktan sonra, istenilen koşullarda kontrollü şekilde salımı, bir süredir pek çok araştırmacının ilgisini çekmektedir. Bu çalışmanın amacı, aljinat (A), karragenan (C), jelatin (G) ve/veya poli (laktik-ko-glikolik asit) (P) bileşenlerden ikisinin (AC, AG, AP), üçünün (ACG, ACP, ACGP) veya dördünün (ACGP) bileşiminden oluşan kompozit mikroboncuklar sentezlemek ve boncukların ilaç salımında kullanılabilirliğini incelemektir. Bu amaçla model ilaç olarak Sefaklor (Cef) antibiyotiği seçilmiştir. Farklı koşullarda sentezlenen, ilaçlı ve ilaçsız kompozit mikrokürelerin Fourier Dönüşümlü Kızılötesi (FTIR) spektrumları karşılaştırılmıştır. Bileşen miktarları, çapraz bağlayıcı iyon miktarları gibi sentez koşullarının şişme, tutulma verimliliği ve malzemelerin salım kinetiği üzerindeki etkileri incelenmiştir. %157-981 (AG-A) oranında en yüksek şişme kapasitesine sahip olan aljinat içerikli mikroboncuklar hidrojel malzemeler olarak tanımlanabilir. Aljinat küresine PLGA eklenmesi şişme kapasitesini azaltırken, diğer bileşenleri içeren kompozit boncuklara PLGA eklenmesi şişme %'sini arttırmaktadır. ACP kürelerine eklenen PLGA miktarı arttıkça şişme azalır. Sefaklorun mikro-kompozitlerde maksimum tutulma etkinliği %36-93 (A-ACP) arasında değişmektedir. Tüm salım deneyleri, çalkalama ortamında yeni çözeltilerle, vücut sıcaklığında, enzimsiz simüle edilmiş mide sıvısında gerçekleştirilmiştir. Sefaklorun kompozit boncuklardan salımında genellikle bir patlama etkisi görülmemiştir. Seçilen veriler, sıfırıncı ve birinci dereceden salım kinetiği ile Korsmeyer Peppas ve Higuchi ilaç salım modellerine uymaktadır.

Anahtar Kelimeler *Sefaklor salınımı; Aljinat; Karragenan; Jelatin; Poli(laktik-ko-glikolik asit)*

1. Introduction

Biocomposite drug carriers are materials that have the potential to contribute to significant advances in pharmacology, improving therapeutic efficacy and sensitivity while minimizing side effects, enabling targeted delivery, and minimizing toxicity in the body. Recent research has focused on bionanocomposite structures based on biopolymers, including lipids (including liposomes, lipid emulsions, lipid nanoparticles, solid lipid nanoparticles, and nanostructured lipid carriers), polysaccharides (including alginate and cellulose), and proteins (e.g., gelatin and albumin)

Sorumlu Yazar / Corresponding Author: Buse SEMERCİ ARIKAN e-posta / e-mail: busesemerci2@gmail.com

(Jamroży et al. 2024). Some of the biomaterials are hydrogels. Hydrogel use in drug release is of interest because it retains and systematically releases drugs, and the higher water content helps encapsulate hydrophilic drugs. The drug can be loaded into the hydrogel in two ways: first, the polymer is combined with the drug, followed by polymerization with crosslinking agents. In the second technique, the hydrogels produced are immediately immersed in the drug solution. Swell-modulated, diffusion-controlled, chemical-controlled, and environmentally sensitive releases are some of the ways the drug is loaded into and released from the hydrogel (Kasai et al. 2022).

One of the preferred antibiotics for drug delivery research is cefaclor. Cefaclor is a second-generation cephalosporin antibiotic. It is more effective against gram-negative bacteria and has antibacterial activity against aerobic gram-positive bacteria and some anaerobes. It is derived from the fungus *Acremonium*, commonly known as Cephalosporium, and is used to treat upper and lower respiratory tract infections, acute sinusitis, otitis media and uncomplicated urinary tract infections. Its qualitative and quantitative analysis is performed using various analytical techniques such as HPLC, HTPLC, capillary zone electrophoresis, UV, IR and NMR spectrometry and UPLC-MS-MS. Depending on the manufacturing and storage conditions, the drug undergoes degradation by oxidation, hydrolysis and racemisation.

Environmental factors such as temperature, oxygen, carbon dioxide, humidity, light and pH accelerate the degradation of the drug. Cefaclor, whose chemical formula is $C_{15}H_{14}Cl\ N_3O_4S$ (MW = 367.812 g mol^{-1}), has a maximum plasma concentration of ~23 µg mL^{-1} with the standard release; and this concentration is reached within ~1 hour (h). Although the plasma half-life is less than 1 h under normal conditions, it increases to 3 h in patients with renal failure and 1.5 h on hemodialysis. The serum half-life ranges from 0.6 to 0.9 h, while the biological half-life ranges from 2.3 to 2.8 h (Arsalan 2017). In the literature, some of the support materials used for the controlled release of cefaclor, one of the β-lactam antibiotics, are: polymethylcyanoacrylate (PECA) nanoparticles (Cavallaro et al. 1994); microspheres composed of polyvinylpyrrolidone and ethylcellulose (EC) dispersed in a solvent mixture (Chow et al. 1998); alginate-based polymer matrices (containing alginate, chitosan, hydroxypropyl methylcellulose [HPMC], lactose, citric acid) (Bak et al. 2002); microspheres made from porcine mucus (soluble mucus glycoprotein, S-mucus) and gelatin, a pharmaceutical polymer of natural origin (Ofokansi et al. 2009); ethyl cellulose (EC), cellulose acetate phthalate (CAP) or shellac-coated chitosan-alginate beads (Rasool and Fahmy 2013); floating microspheres composed of HPMC K4M and ethyl cellulose prepared by emulsion solvent evaporation technique (Chilukala et al. 2016); poly(ethyl acrylate, methyl methacrylate and chloro-trimethyl-ammonio-ethyl methacrylate) (ERS) copolymer nanoparticles prepared by conventional spray drying device (Öztürk and Aygül 2020); chitosan, PVA and hydroxyapatite based hydrogel mixtures etc. (Faizan 2024). The last table (in section 3.5) lists the experimental conditions and results of some of the studies mentioned above and compares them with those of the present study. Various new technologies such as microspheres, improved formulations and new drug delivery systems, including extended-release cefaclor tablets, provide protection against degradation and help improve the bactericidal effect and pharmacokinetic profile of the drug (Arsalan et al. 2017). The main aim of this study is to use biomaterials that do not contain toxic substances and can be synthesised in a simple and practical way for the release of a model antibiotic. In Semerci Arıkan's master's thesis, two-component (AC, AG), three-component (ACG, ACP, AGP) and four-component (ACGP) composite beads consisting of different combinations of alginate and carrageenan (A and C, high molecular weight polysaccharides), gelatin protein (G) and/or poly(lactic-co-glycolic acid) (P, a biodegradable polymer) were synthesised, characterised by different methods and used for the release of cefaclor (Semerci, 2019). The characterisation of composite microbeads was presented in another article with the contribution of density functional theory (DFT) calculations (Baybaş et al. 2021).

This article focuses on the above-mentioned AC, AG and ACG beads and their composites formed with PLGA (ACP, AGP, ACGP), cefaclor loading via co-synthesis (bead-Cef) and the usability of the beads for cefaclor release at simulated gastric pH without pepsin. As cefaclor is known to be unstable at intestinal pH (Rasool et al., 2013; Kolesynk et al., 2015) and alginate-containing composites are also unstable under these conditions, the release studies were only performed at pH = 1.2. The presence of cefaclor in the structure was revealed by comparing the FTIR spectra in the study. The swelling behaviour of the microspheres was also investigated. It was observed that the prepared composite beads were hydrogels with high swelling capacity. The study has primarily guided a graduate student towards research. If supported by studies to improve materials and include in vivo experiments, it could also contribute to the country's economy in the field of pharmacology.

2. Materials and Methods

2.1. Materials

In the study, sodium alginate (A; Carlo Erba, France), carrageenan (C; Sigma-Aldrich, USA), gelatin (G; Merck, Germany) and poly(lactic-co-glycolic acid) (P, resomer, ®RG 503 H, PLGA, lactide glycolide (50:50, MW 24,000-38,000; Sigma-Aldrich, Germany) were used as composite components. Poly(vinyl alcohol) (PVA; Sigma-Aldrich, USA) was used as an emulsifier to form PLGA particles. The cross-linking salts used to form alginate and carrageenan beads were calcium chloride ($CaCl_2.2H_2O$; Carlo Erba, France) and potassium chloride (KCl; Tekkim, Turkey). Cefaclor, an antibiotic belonging to the cephalosporin class, was chosen as the model drug for delivery/release experiments. Pure cefaclor was provided free of charge by Centrient Pharmaceuticals (DSM Sinochem Pharmaceuticals, Rotterdam, The Netherlands). Buffer solutions were prepared using monosodium phosphate (NaH_2PO_4; Sigma-Aldrich, Germany), disodium phosphate (Na_2HPO_4; Sigma-Aldrich, Germany), trisodium phosphate (Na_3PO_4; Merck, Germany) and HCl (Merck, Germany) to provide a gastric pH medium. The analytical purity of all chemicals and double-distilled water used to prepare the solutions in this study was maintained.

2.2. Synthesis of Alginate-Containing Spheres

The synthesis of composite beads by the ionic gelation method was performed using procedures similar to those used in previous publications (Kolesnyk et al. 2015, Torres et al. 2011, Popa et al. 2011). The synthesis conditions for alginate-containing polymeric beads are presented in Tables 1-3. In the tables, the first section, the gel medium, included the volume of water or drug solution (V/mL), the drug concentration in ppm (Cef/µg mL^{-1}) and the mass of polysaccharide (mA, mC), gelatin (mG) and PLGA (mP) in mg. The other section, the bead medium, contained the mass/volume percentages of KCl-$CaCl_2$ salts and PVA in the same volume. More detailed information on the synthesis of drug-free micro-composites can be found in Semerci 2019 and Baybaş et al. 2021.

For the synthesis of beads without PLGA (A, AC, AG and ACG in Table 1), the gels formed by dissolving the components alginate (A), carrageenan (C) and gelatin (G) in water (gel medium) were dropped into the precipitation solution containing $CaCl_2$ and KCl (bead medium) using a syringe. For the synthesis of gels with PLGA (AP, ACP, AGP and ACGP in Table 2), the PLGA solution in acetone was added to the gels containing A, C and G. After mixing the gel solutions until they were homogeneous and evaporating the acetone (gel medium), they were dropped with a syringe into the solution containing $CaCl_2$, KCl salts and polyvinyl alcohol (PVA), resulting in spherical structures (bead medium).

Table 1. Synthesis conditions of micro-beads without PLGA used in swelling experiments

Sample Codes	Gel Medium				Bead Medium	
	V	m_A	m_C	m_G	KCl	$CaCl_2$
	Ml	mg	mg	mg	%	%
A	15	300	-	-	1.0	1.0
AC	10	100	100	-	2.5[1]	3.3[2]
AG	15	150	-	150	1.0	1.0
ACG	15	100	100	100	1.0	1.0

[1]%(Mass/Volume)= 2.5% equivalent 0.3 mol L^{-1} KCl
[1]%(Mass/Volume)= 3.3% equivalent 0.3 mol L^{-1} $CaCl_2$

Spheres containing cefaclor (A-Cef, AC-Cef, AG-Cef, ACG-Cef, AP-Cef, ACP-Cef, AGP-Cef and ACGP-Cef in Table 3) were prepared by co-synthesis, with the gel medium containing cefaclor solution instead of distilled water. Blind trials showed that acetone did not affect the drug concentration in the PLGA beads. To harden and stabilize all the beads, stirring was continued for 2 hours, then the beads were washed with distilled water and stored in the refrigerator. The sizes of the beads dried under laboratory conditions were in the range of 600-1000 micron sieves and were therefore called "microbeads".

2.3. The FT-IR Analysis of Beads with Drug and Drug-Free

The FT-IR spectra (Figure 1) of some of the drug and non-drug beads that were offered the above synthesis conditions were obtained using the KBr pellet technique and the Fourier transform infrared spectrometer (BRUKER TENSOR II) (Baybaş et al. 2021).

2.4. Swelling Experiments

The swelling tests consist of two main parts. First, the swelling properties of the alginate-carrageenan (AC and ACP) composite beads (without and with PLGA) chosen as examples were compared. Then, swelling kinetics experiments were performed with ACP beads in different pH environments (gastric pH, intestinal pH, distilled water and basic pH). Tables 1 and 2 show the synthesis conditions for these composites. In addition, the effect of the synthesis conditions of the ACP beads on their swelling properties was investigated. The amounts of salts (KCl, $CaCl_2$) in the bead medium were varied in the ACP, ACP1-4, and the weight of PLGA (mP) in the gel medium in the ACP3, ACP5-8 coded samples (Table 2). The swelling properties of alginate (A), alginate-gelatine (AG), alginate-carrageenan-gelatine (ACG) and their composites with PLGA (AP, AGP, ACGP) in water were then investigated. The synthesis conditions of these composite spheres are shown in Tables 1 and 2.

Table 2. Synthesis conditions of micro-beads with PLGA used in swelling experiments

Sample Codes	Gel Medium					Bead Medium		
	V/ mL	m_A/ mg	m_C/ mg	m_G/ mg	m_P/ mg	KCl / %	$CaCl_2$ / %	PVA %
ACP	15	100	100	-	*50*	2.5	3.3	3
ACP1	15	100	100	-	50	*0.5*	*0.5*	3
ACP2	15	100	100	-	50	*1.0*	*1.0*	3
ACP3	15	100	100	-	50	*2.0*	*2.0*	3
ACP4	15	100	100	-	50	*5.0*	*5.0*	3
ACP5	15	100	100	-	*20*	2.0	2.0	3
ACP6	15	100	100	-	*100*	2.0	2.0	3
ACP7	15	100	100	-	*200*	2.0	2.0	3
ACP8	15	100	100	-	*400*	2.0	2.0	3
AP	15	*300*		-	*100*	1	1	1
AGP	15	*150*	-	*150*	*100*	1	1	1
ACGP	15	*100*	*100*	*100*	*100*	1	1	1

In all swelling experiments, specific masses of dry beads were weighed at weighing sensitivity and placed into the relevant solution medium, and then the timing was started. The spheres were removed from the environment at certain times, dried in a way that removes the surface water, and weighed. Swelling kinetics plots were presented in Figures 2-5.

2.5. Release Experiments at Gastric pH

Table 3 shows the synthesis conditions of the composite beads used in the release experiments. The specific masses of all synthesized samples (with and without cefaclor) were weighed. Then, 5 mL of the sample was placed in a simulated gastric environment (without enzyme) at pH 1.2 and kept in a shaking incubator at 36 oC for a specified time. It was then removed from this environment and placed in a new 5 mL acidic environment. At the end of the experiment, the cefaclor concentrations of all waste (released) solutions were measured using a UV-Vis spectrophotometer (Shimadzu/UV-1800) (example of a calibration curve in Figure 6) and the cumulative release results were plotted against time (Figures 7-9).

3. Results and Discussion

3.1 Data Analysis

Analysis of swelling behavior is one of the most commonly used methods for characterizing polymers, especially hydrogels. The degree of swelling of the composite beads at any given time can be calculated using a known equation.

$$S = \frac{(m_t - m_0)}{m_0} \quad (1)$$

In equation (1), m_t is the mass of beads removed from the release medium at any time (t), while m_0 is the dry bead mass. This equation can be used to determine the degree of swelling (S) of the composite beads; the percentage swelling (S %) values can be calculated by multiplying the equation by 100. In this study, the value with the highest S % is shown as S_{max} % and taken as the maximum percentage swelling value (Table 4). Schott's second order swelling kinetics equation applies to high swelling polymers (Table 5):

$$\frac{t}{S} = A + Bt \quad (2)$$

$A = \frac{1}{kS_e^2}$, indicates the inverse of the swelling rate in the first case (min g bead g^{-1} water) and $B = \frac{1}{S_e}$, indicates the inverse of the maximum or equilibrium swelling value (S_e) (g bead g^{-1} water). Here, k indicates the swelling rate constant (g water g^{-1} bead min^{-1}) (Schott 1992). Concentrations of cefaclor are easily determined without complexing agents using a UV-Vis spectrophotometer. As there may be shifts in the maximum wavelength of the drug in media of different pH and ionic strength (distilled water, simulated gastric fluid without enzymes), wavelength scans and calibration graphs were plotted separately for each medium. In the synthesis of drug-loaded beads and release studies, one of the components of the composite may interfere with the maximum wavelength of the drug. To eliminate this possibility, beads with and without cefaclor were synthesized simultaneously; wavelength scans of the fluids (background) were performed during the synthesis of the non-drug beads and no interference was found. The UV-Vis spectra (maximum absorbance peaks at 264 nm and 268 nm, no peak) were obtained for Cefaclor in both media, together with that of the background, and the sample calibration graphs are shown in Figures 6a and b. Calibration curves were plotted before each analysis and the calibration curve parameters were found to be repeatable and reproducible. The entrapment efficiency percentage (EE%) of the beads was calculated prior to the composite release tests and the values obtained are shown in Table 6 together with the release values. The EE% was calculated using the following equation (3).

Table 3. Synthesis conditions of micro-beads with or without the drug, used in release experiments

Sample Codes	Gel Medium						Bead Medium		
	V/ mL	$m_{A/}$ mg	$m_{C/}$ mg	$m_{G/}$ mg	$m_{P/}$ mg	*Cef/ µg mL^{-1}*	KCl%	$CaCl_2$%	PVA%
AC-Cef1	10	100	100	-	-	*50*	*2.5*	*3.3*	-
AC-Cef2	10	100	100	-	-	*250*	*2.5*	*3.3*	-
AC-Cef3	10	100	100	-	-	*500*	*2.5*	*3.3*	-
AC-Cef4	10	100	100	-	-	*1000*	*2.5*	*3.3*	-
AC-Cef5	10	100	100	-	-	*5000*	*2.5*	*3.3*	-
AC	10	100	100	-	-	-	*2.5*	*3.3*	-
AC-Cef	10	100	100	-	-	250	*2.5*	*3.3*	-
AC1	10	100	100	-	-	-	*1*	*1*	-
AC1-Cef	10	100	100	-	-	250	*1*	*1*	-
AC2	10	100	100	-	-	-	*2*	*2*	-
AC2-Cef	10	100	100	-	-	250	*2*	*2*	-
AC3	10	100	100	-	-	-	*3*	*3*	-
AC3-Cef	10	100	100	-	-	250	*3*	*3*	-
A	15	*300*	-	-	-	-	1	1	-
A-Cef	15	*300*	-	-	-	250	1	1	-
AC4	15	*200*	*100*	-	-	-	1	1	-
AC4-Cef	15	*200*	*100*	-	-	250	1	1	-
AP	15	*300*	-	-	100	-	1	1	1
AP-Cef	15	*300*	-	-	100	250	1	1	1
ACP9	15	*200*	*100*	-	100	-	1	1	1
ACP9-Cef	15	*200*	*100*	-	100	250	1	1	1
ACP10	10	100	100	-	*50*	-	2.5	3.0	*1*
ACP10-Cef	10	100	100	-	*50*	250	2.5	3.0	*1*
ACP11	10	100	100	-	*100*	-	2.5	3.0	1
ACP11-Cef	10	100	100	-	*100*	250	2.5	3.0	1
ACP12	10	100	100	-	*200*	-	2.5	3.0	1
ACP12-Cef	10	100	100	-	*200*	250	2.5	3.0	1
ACP13	10	100	100	-	100	-	2.5	3.0	*3*
ACP13-Cef	10	100	100	-	100	250	2.5	3.0	*3*
ACP14	10	100	100	-	200	-	2.5	3.0	-
ACP14-Cef	10	100	100	-	200	250	2.5	3.0	-
A	15	*300*	-	-	-	-	1	1	-
A-Cef	15	*300*	-	-	-	250	1	1	-
AG	15	*150*	-	*150*	-	-	1	1	-
AG-Cef	15	*150*	-	*150*	-	250	1	1	-
AG1	15	*200*	-	*100*	-	-	1	1	-
AG1-Cef	15	*200*	-	*100*	-	250	1	1	-
AP	15	*300*	-	-	100	-	1	1	1
AP-Cef	15	*300*	-	-	100	250	1	1	1
AGP	15	*100*	-	*100*	100	-	1	1	1
AGP-Cef	15	*100*	-	*100*	100	250	1	1	1
AGP1	15	*200*	-	*100*	100	-	1	1	1
AGP1-Cef	15	*200*	-	*100*	100	250	1	1	1
ACG	15	*100*	*100*	*100*	-	-	1	1	-
ACG-Cef	15	*100*	*100*	*100*	-	250	1	1	-
ACG1	15	*200*	*50*	*50*	-	-	1	1	-
ACG1-Cef	15	*200*	*50*	*50*	-	250	1	1	-
ACGP	15	*100*	*100*	*100*	100	-	1	1	1
ACGP-Cef	15	*100*	*100*	*100*	100	250	1	1	1

$$\text{EE } \% = \frac{\left(C_0 x \frac{m_b}{m_g}\right) - C_w}{C_0 x \frac{m_b}{m_g}} x100 \qquad (3)$$

Here, C_0 refers to the drug concentration added at the beginning (µg mL^{-1}); C_w refers to the drug concentration (µg mL^{-1}) that comes after washing; m_b refers to the total mass of the synthesized beads, and m_g refers to the mass of the homogeneous gel without forming beads.

For the synthesized composites, release kinetics studies were performed at gastric pH (HCl at pH 1.2) and the variation of the total and percentage release rate of cefaclor, a drug-loaded composite, over time was investigated. All procedures in the release experiments

were also carried out for the inert beads and the absorbance of the solutions obtained was measured as a blank. As indicated in the relevant parts of section 2 (Experimental procedure), partial (fractionated) release experiments were performed using a fresh solution for each period and the total (cumulative) release values were calculated.

Equations (4) and (5) were used in total (ΣR) and percent release (R%) calculations.

$$\Sigma R = \frac{\Delta C.V}{m} \quad (4)$$

In this equation, $\Delta C = C_{Cef} - C_0$; C_0 is the blank concentration value (usually close to zero) calculated from the calibration during the release of the beads without drug (blank); C_{Cef} is the drug concentration (ppm, μg mL^{-1}) calculated during the release of Cefaclor; and V is the volume of HCl added to the release medium (mL), while m is the initial weighed mass (g) of the bead whose release kinetics is being studied. Accordingly, the release value is expressed in the following unit μg drug (g dry bead)-1 released.

$$R\,\% = \frac{\Sigma R}{EE} 100 \quad (5)$$

In this equation, the percentage release (Release %) is calculated as the ratio of the total release value found using equation (4) to the amount of drug loaded on the initial dry bead (μg Cef/g initial dry bead) calculated using equation (3) and is expressed in the unit of μg drug released/initial μg drug (Table 6).

Several release kinetics models have been developed for controlled drug delivery systems. Drug release profiles have been generated using the amount of drug released from drug delivery systems as a function of time (Table 7). The models developed for drug release kinetics include the following.

- Zero-order kinetics
- First-order kinetics
- Higuchi model
- Hixson-Crowell model
- Korsmeyer-Peppas model
- Baker– Lonsdale model
- Hopfenberg model

In this study, the zero-order, first-order, Higuchi and Korsmeyer-Peppas models were applied to the release kinetics data of some composites that showed a high release rate at gastric pH. The mathematical formulae developed for these release kinetics models are as follows:

- Zero-order kinetics formula

$$M_t/M_\infty = k_0\, t \quad (6)$$

- First-order kinetics formula

$$\log(1- M_t/M_\infty) = k_1\, t \quad (7)$$

- Korsmeyer-Peppas equation

$$M_t/M_\infty = k\, t^n \quad (8)$$

- Higuchi equation

$$M_t/M_\infty = k_H \sqrt{t} \quad (9)$$

In these equations, M_t is the amount of drug released at the time (t), M_∞ is the initial amount of drug, and t is the release time.

In equation (6), k_0 is the zero-order proportional constant. This method is generally used for drugs with low solubility. The amount released is determined by plotting the drug released as a function of time (Dash et al. 2010).

If $M_t/M_\infty = F$ in equation (7), then F is the drug release fraction. While k_1 is the first order rate constant in unit $time^{-1}$, t is the release time. This model is used to describe drug entrapment and absorption. The amount of drug dissolved (released) in the dosage form is determined. It is commonly used to determine the amount of water-soluble drugs (Dash et al. 2010).

In equation (8), k is a characteristic constant for the drug, n is the diffusion exponential and t is the release time. The calculated value of n is used to explain the different release mechanisms. A value of n close to 0.5 indicates that the structure fits Fick's law, while a value of n greater than 0.5 indicates that the drug release is in a structure that fits the non-Fick model. When the release form is a cylinder, the reference value for the n value is 0.45 instead of 0.5 (Dash et al. 2010, Karadağ et al. 2016).

Finally, in Eq. (9), k_H is the release rate constant, which includes the parameters of the polymer structure, and t is the release time. This is the most commonly used method among release kinetics models. In this method, drug release is determined by plotting against the square root of time (Dash et al. 2010).

3.2 The FT-IR Spectra of Beads with Drug and Drug-Free

The authors presented these FT-IR, TGA/DSC, SEM and PZC analyses of beads in a previous study (Baybaş et al. 2021). Here, only the sample FT-IR spectra of drug and non-drug beads are compared. The FT-IR spectra of PLGA (AC, AG, ACG) and PLGA (ACP, AGP, ACGP) composite beads with and without the drug are compared in Fig. 1. The spectrum of cefaclor is also shown in Figures 1a and b. OH and amide NH stretching from broadband series H2O seen in the range of 3680-3000 cm^{-1} in the FTIR spectrum, broadband CO_2 at 2580 cm^{-1}, strong band β-lactam C=O stretching at 1775 cm^{-1}, strong band amide

C=O stretching at 1693 cm^{-1}, strong band carboxylate stretching at 1600 cm^{-1}, weak bands at 1560 cm-1 and moderate bands at 1500 cm^{-1} aromatic C=C, the strong band at CO_2- (symmetrical) at 1365 cm^{-1} defines the sharp peak C-Cl bond at 697 cm^{-1} (Lorenz et al. 1980).

The bands at 1628 and 1425 cm^{-1} observed in the upper AC spectrum in Figure 1a belong to the asymmetric and symmetric carboxyl group strains at 1613 and 1418 cm^{-1} characterized for A. In addition, the shoulder of the C-O bond seen in the alginate spectrum at 1127 cm^{-1} is seen in the AC spectrum at 1127 cm^{-1}. 1262 cm^{-1} SO_3^- group strain of C at 1261 cm^{-1} in the composite; C-O cyclic stretching at 1160 cm^{-1} at the same wavenumber; C-O-C cyclic ether absorption bands at 1070 and 1041 cm^{-1} are located at 1068 and 1041 cm^{-1} in the composite. In addition, low-intensity bands at 973, 930 and 847 cm^{-1} in C are present at 969, 930 and 847 cm^{-1} in AC (Mishra 2015). The differences between AC and ACP composites (Figure 1b) in the region between 1340-1140 cm^{-1} and 1148-950 cm^{-1} prove that PLGA is included in the structure (Sun et al. 2015). It indicates that AC composite beads are a new structure consisting of A and C components and ACP composite beads are a new structure consisting of A, C and P components. When AC and AC-Cef spectra (Figure 1a) are examined with the same graph and similarly ACP and ACP-Cef spectra (Figure 1b), there is no new peak formation or complete disappearance. The retraction of the bands may indicate the interaction between Cefaclor and the composite total functional groups

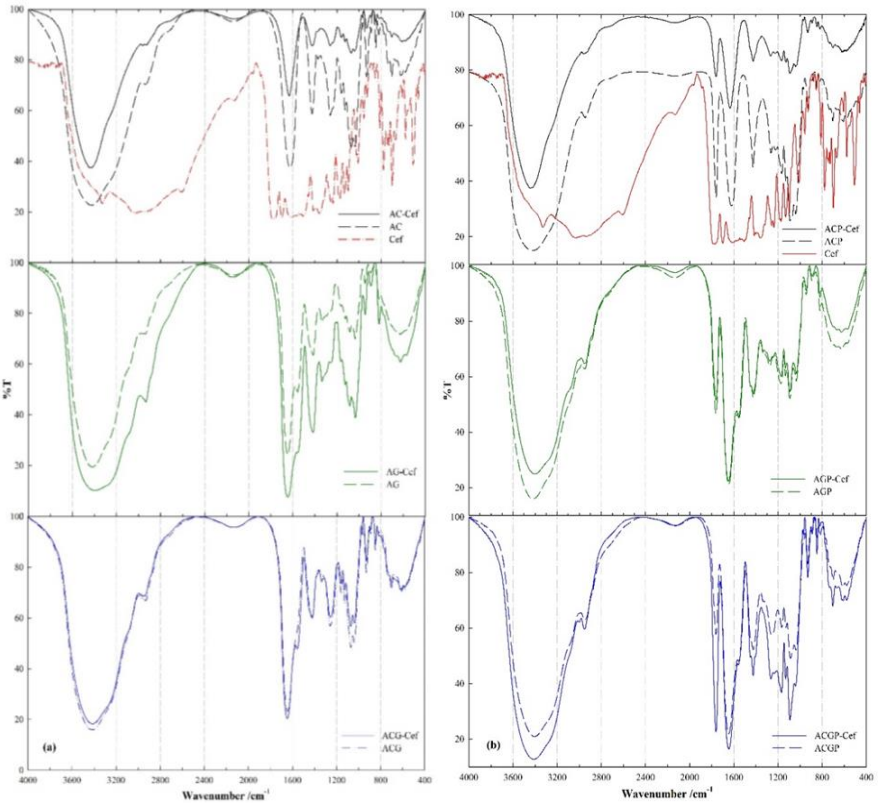

Figure 1. FT-IR spectra of Cef and (a) with PLGA beads, (b) without PLGA beads.

Similarly, only the width of the O-H band is comparable in the group frequency domain for AG. This band is a combination of broad A and narrow G bands. According to Mishra (2015), the fingerprint region for gelatine is in the range of 1650-800 cm^{-1} (Mishra 2015). The amide bands of 1639, 1545 and 1337 cm^{-1}, characterised for G in this region, are seen at 1648, 1556 and 1336 cm^{-1} in the AG composite. The characteristic carboxyl group peaks of alginate at 1613 and 1418 cm^{-1} were also observed in the composite at 1648 (overlap) and 1416 cm^{-1}. In addition, the band with shoulders in the range of 1230-960 cm^{-1} in the alginate spectrum is also seen in the composite with lower intensity. This region also includes the 1336 cm^{-1} peak of G. When the spectra of AG-Cef and AG-coded beads with or without cefaclor are examined, in contrast to the previous figure, there is an elongation in the bands of the active composite. In the spectrum of AG-Cef, the band at 625 cm^{-1}, which is different from AG, may be evidence of cefaclor binding.

When the spectra are looked at holistically, it is understood that the ACP composite interacts most with Cefaclor. The entrapment efficiency also evidences this in Table 6.

3.3 Swelling Tests

3.3.1 The Effect of the Presence of PLGA on Swelling (AC/ACP Beads)

The swelling kinetics of AC and ACP composites in water, whose synthesis conditions are seen in Tables 1 and 2, were compared, and the effect of the presence of PLGA on swelling was investigated (Figure 2a). The swelling capacity of the AC and ACP gels reached the highest value (442% and 466%) at 45 and 60 minutes, respectively. As with all swelling kinetics graphs, this figure exhibits both swelling and syneresis (de-swelling). The rapid decline observed after a certain period can be attributed to the stripping of carrageenan from the composite structure (erosion) and then to the degradation of the entire structure. Because the carrageenan can form a gel not only with 1- and 2-valued cations but also with temperature, this process is reversible.

On the other hand, Alginate can form a gel only with 2-valued cations, and the process is not thermally reversible. However, in the studies of Davidovich-Pinhas and Bianco-Peled both swelling and syneresis were observed in alginate-containing structures. The authors reported this was due to the G (α-L-guluronic-acid) content and Ca^{2+} concentration (Davidovich-Pinhas and Bianco-Peled 2010).

Furthermore, adding PLGA to the composite slightly increased the maximum swelling value and the time required to reach this value. Since there is no significant swelling difference between the AC and ACP composites, the following swelling experiments were performed with the ACP composites.

3.3.1.1 Variation of Swelling with pH

Figure 2b shows the %Swelling-t plots for the ACP coded beads at laboratory temperature and placed in distilled water, gastric pH (pH = 1.2 HCl solution), intestinal pH (pH = 7.4 phosphate buffer, PB) and basic pH (pH = 10.0 NaOH). This sample was chosen because it is the bead with the best homogeneity and physical appearance. After some time, bead breakage and mass loss were observed at all pH values and equilibrium swelling values could not be measured. The highest swelling value (Sm%) for the four different pH environments was > 100 and the highest swelling occurred in water.

The maximum swelling values were 536% after 45 minutes in water, 253% after 30 minutes in HCl, 195% after 15 minutes in phosphate buffer and 186% after 20 minutes in NaOH (Table 4). These different degrees of swelling demonstrated that the ACP beads were pH sensitive.

Table 4. Examples of the swelling test, calculated maximum Swelling% values, and time to achieve this value

Composites	$(S\%)_{max}$	t_{max}/min
Without PLGA		
A	981	45
AC	442	45
AG	157	120
ACG	618	60
With PLGA		
AP	747	180
ACP	464	60
AGP	295	180
ACGP	641	180

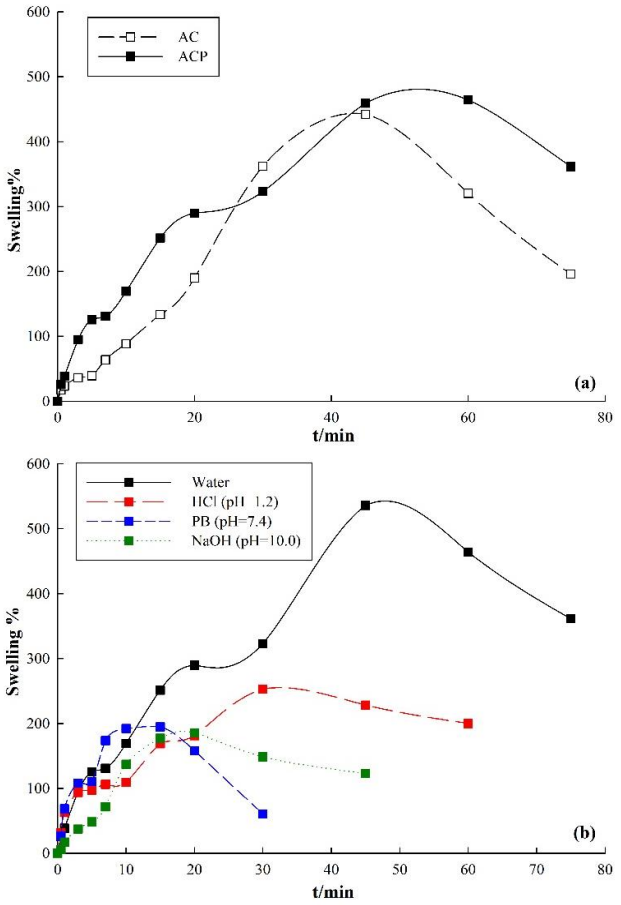

Figure 2. (a) Swelling kinetics of alginate-carrageenan (AC) and alginate-carrageenan-PLGA (ACP) composites at room temperature and in water, **(b)** swelling kinetics of ACP at different pH conditions.

The literature also suggests that alginate beads swell more and are more stable at gastric pH than at intestinal pH. In a study investigating the effect of pH on the swelling values of alginate beads prepared in the presence of Ba^{2+} and Ca^{2+}, hydrogen bonding was reported as the reason for the stability at acidic pH. According to the authors, the pK_a values of the mannuronic and guluronic acid residues of alginate were 3.38 and 3.65, respectively. At a pH below the pK_a of uronic acid, alginate gels are stabilized by intermolecular hydrogen bonding. This is why alginate particles degrade readily in the intestine but are stable in the gastric

environment. The high swelling rate can be attributed to chain expansion at a higher pH than the ionic carboxylate groups of the alginate (Chuang 2017). In addition, the lower degree of swelling in the acidic medium is also explained by the stronger polymer-polymer interactions than polymer-solvent interactions due to the hydrogen bonds formed between the unresolved carboxyl groups in the alginate (Kolesnyk 2015). As the beads were found to be unstable at phosphate buffer and basic pH, subsequent swelling experiments were performed at gastric pH and/or distilled water.

3.3.2 Swelling Properties of the ACP Beads

Firstly, the swelling properties of the ACP-encoded beads, whose synthesis conditions are given in Table 2, were studied in different pH environments. Then, the swelling kinetics of the composite beads prepared under different synthesis conditions (different amounts of KCl and $CaCl_2$ and different PLGA contents) were studied.

3.3.2.1 The Change in Swelling with the Amount of Salt in the Bead Synthesis Medium

Figure 3 (a and b) shows the %Swelling values of ACP and ACP1-4 encoded beads, whose synthesis conditions are given in Table 2, at ambient temperature in HCl and water, respectively. The synthesis conditions show that these composites contain 50 mg of PLGA with equal mass (100 mg) of A and C. For all composites, 3% PVA and varying amounts of salt (KCl and $CaCl_2$) were present in the bead-forming medium. As shown in Figure 3b, ACP was synthesized in environments with different salt ratios (% m/V) (0.3 mol L^{-1} KCl and $CaCl_2$ ≡ 2.5% KCl and 3.3%; $CaCl_2$; can be considered as approximately 3% salt). The swelling kinetics of ACP1 (0.5%), ACP2 (1%), ACP3 (2%) and ACP4 (5%) beads were studied (a) at gastric pH and (b) in water.

The bead with the highest swelling in water was ACP1 (0.5% KCl and $CaCl_2$) (Table 4). This is an expected result considering that the salts have a cross-linking function. However, this is not the case at gastric pH where the ACP1 bead is unstable for long in water and HCl and tends to disintegrate. Although the swelling of the composites in water was higher than in an acidic environment, the beads without degradation had shorter stabilities. Since the beads synthesized in 1% (ACP2) and 2% (ACP3) salt medium at both pH conditions had better stability than those synthesized in other salt ratios, 0.5% and 5% salt environments were not used in the subsequent synthesis processes. It can also be said that ACP (approximately 3% salt) and ACP3 (2% salt) show similar swelling kinetics at gastric pH.

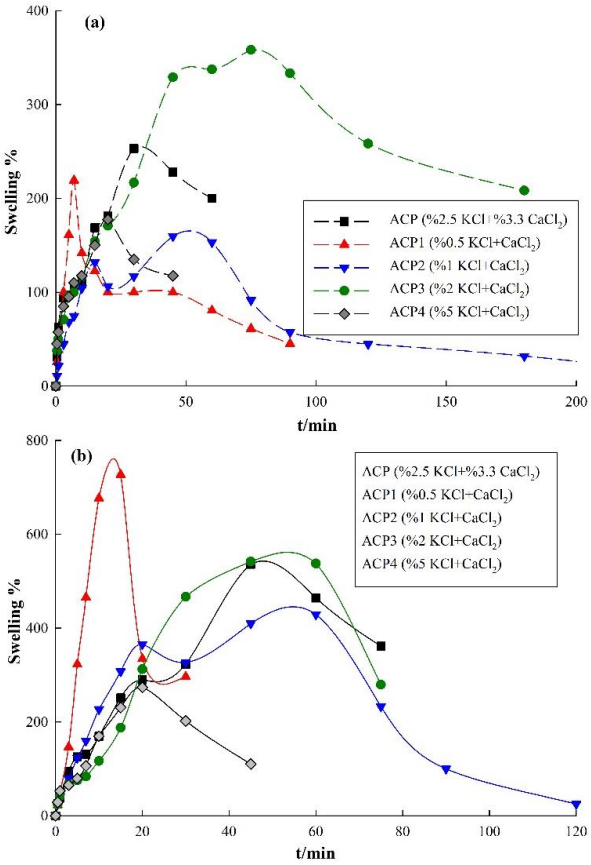

Figure 3. Swelling kinetics of the beads synthesized in different salt environments (a) at gastric pH and (b) in water.

3.3.2.2 The Change in Swelling with the Amount of PLGA added to the Gel

After investigating the effect of alginate-carrageenan mass and salt amount on bead formation and swelling, the effect of PLGA mass was investigated. The A and C masses were chosen as 100 mg, the salt content in the precipitation medium as 2%, and the PVA content as 3%, and then composite beads containing PLGA with different masses were formed (Table 2). Figure 4 shows the %Swelling values of these ACP4 and ACP5-8 coded beads at ambient temperature in (a) HCl and (b) water. Comparing the swelling and stability times in both pH mediums indicates that the ACP3 beads containing 50 mg PLGA showed the best performance. The homogeneous and opaque appearance of these beads has also confirmed this situation.

Adding the hydrophobic PLGA polymer to the environment is expected to reduce swelling. Figures 2(b) and 3 show that the swelling values were higher in water than in acid in Figure 4.

3.3.3 Swelling Properties of the A, AG, ACG, AP, AGP and ACGP Beads

Figure 5 shows the swelling kinetics in water at an ambient temperature of the double and triple (AG, ACG)

composites without PLGA and the triple and quadruple (AGP and ACGP) composites with PLGA, except the AC and ACP. Since the swelling kinetics of the AC and ACP beads were previously presented in Figure 2(a) and the amount of salt in the synthesis conditions was different, they were not included in this comparison.

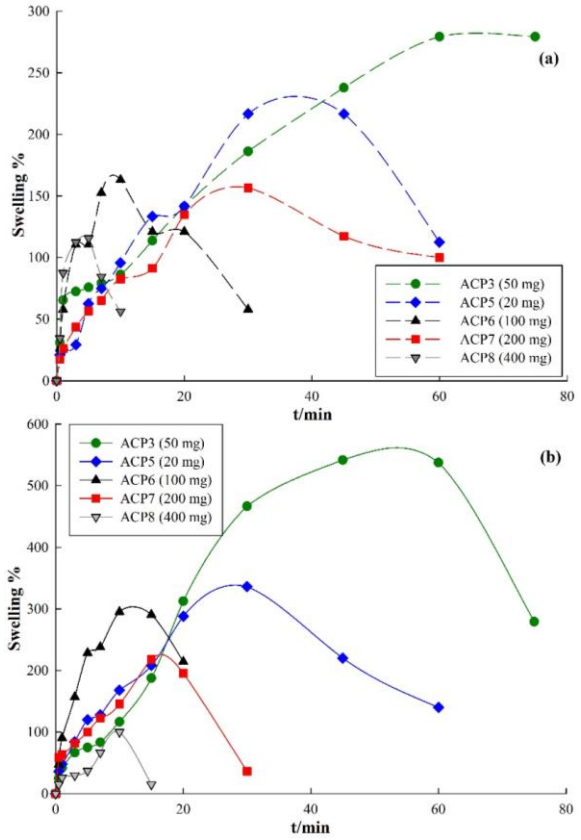

Figure 4. Swelling kinetics of the beads with different PLGA masses in **(a)** gastric pH and **(b)** water.

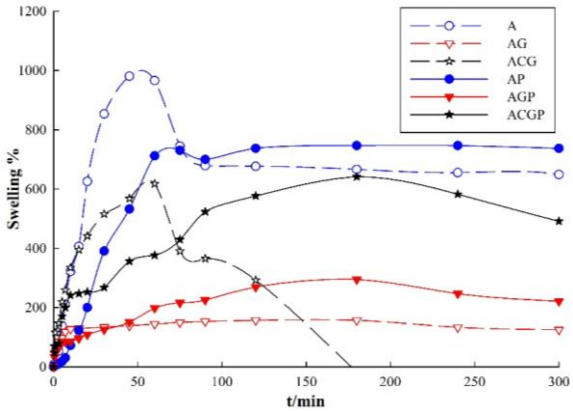

Figure 5. Water swelling kinetics of the beads prepared under the same conditions: alginate (A), alginate-gelatin (AG), alginate-carrageenan-gelatin (ACG), and alginate-PLGA (AP), alginate-gelatin-PLGA (AGP), alginate-carrageenan-gelatin-PLGA (ACG).

A decrease in the mass (syneresis) of the beads without PLGA, except AG (A, ACG), was observed before the end of the 1 hour. In Figure 2a, the rapid decrease in the swelling capacity of the AC gel after reaching the highest value at 45 min can be explained by removing the carrageenan from the composite structure (erosion) and the subsequent degradation of the whole structure. Compared to Figure 4, the gelatine incorporated into the environment reduced this characteristic in A and C and increased the swelling.

The PLGA added to the beads further reduced this degradation property. Investigation of the contribution of PLGA to swelling showed that when added to alginate it increased cross-linking, preventing the alginates from dissolving and reducing swelling. The addition of PLGA to AC (Figure 3a), AG and ACG had the opposite effect and increased swelling. As mentioned above, the hydrophobic nature of PLGA would be expected to reduce swelling. However, all composites can be considered as reversible hydrogels without covalent bonds. In other words, the physical network structures are held together by ionic interactions between polymer chains, hydrogen bonds and/or van der Waals interactions and exhibit a reversible structure. A review by Lin and Metters (Lin et al. 2006) reported that instability and rapid degradability were the common drawbacks of gels formed by physical cross-linking. Adding a hydrophobic group to the structure sometimes prevents water from entering the composite, although sometimes it facilitates water uptake by increasing porosity.

Table 4 shows the maximum percentage swelling values of all the beads whose swelling kinetics were studied at ambient temperature and in water, as well as the times required to reach this value. As can be seen from the table and all the swelling kinetics graphs, all the composite beads containing alginate had a swelling capacity greater than 100%, indicating that all the composites had super-adsorbent hydrogel properties. The degree of swelling of the hydrogel is influenced by van der Waals forces, electrostatic interactions, hydrophobic interactions and hydrogen bonding, while the swelling rate depends on various physicochemical parameters such as porosity and pore structure types. Accordingly, hydrogels are classified into four types as super-porous, macro-porous, micro-porous and non-porous hydrogels (Kasai, et al. 2022). Accordingly, the maximum swelling comparison of the hydrogel composites is A (981%) > AP (747%) > ACGP (641%) > ACG (618%) > ACP (464%) > AC (442%) > AGP (295%) > AG (157%).

In the present study, the difference in swelling between alginate and alginate-carrageenan spheres was contrary to the difference found by Kolesnyk et al. (2015), i.e. AC spheres swelled more than A. The authors stated that this was due to the increase in the amount of κ-carrageenan in the polymer mixture and the decrease in the cross-

linking density due to the increased molar mass of the cross-linked molecules (Kolesnyk et al. 2015). This situation was observed in the present study because the A and AC spheres were prepared in different salt environments.

As can be seen in Table 4, increasing the carrageenan content in the polymer mixture resulted in an increase in the molar mass between the cross-links and a decrease in the cross-link density, which promoted an increase in the degree of swelling of the films. This can be explained by the formation of interlocking networks between the alginate and carrageenan molecular chains, which minimizes the possibility of two adjacent carboxyl groups interacting with Ca^{2+}.

3.3.4 The Second Order Swelling Kinetics Model

Table 5 shows the fit of the beads to Schott's second-order swelling kinetics model and the coefficients obtained from equation (2). The mean and standard deviation (SD) values of the experimental equilibrium swelling data in Figures 2 to 5 are given in the last column of the table. As can be seen in Table 5, the R^2 values of all beads at certain time intervals were very close to 1 and fit the second-order kinetic model. The AC, ACG and ACP beads failed to reach the equilibrium swelling value. The equilibrium swelling values (S_e) obtained using the equation were also compatible with the experimental equilibrium swelling values $(S_e)_{exp}$.

Table 5. Compliance of the PLGA and PLGA composite beads to second-order swelling kinetics model

Composites	R^2	A	B	K	S_e	$(S_e)_{exp}$±SD
Without PLGA						
A	0.987	0.039	0.15	0.58	6.64	6.65±0.13
AC	0.998	1.93	2.16	2.41	0.46	Not
AG1	0.999	2.62	0.62	0.15	1.60	1.40±0.13
ACG1	0.999	1.70	0.14	0.019	7.36	Not
With PLGA						
AP	0.975	0.20	0.14	0.10	6.93	7.18±0.44
ACP1	0.956	3.70	0.15	$6.38x10^{-3}$	6.51	Not
AGP1	0.946	9.73	0.31	$9.67x10^{-3}$	3.26	2.52±0.31
ACGP1	0.967	3.196	0.17	$9.22x10^{-3}$	5.82	5.63±0.58

3.4 Entrapment Efficiency of Cefaclor in Composites and Release Kinetics at Gastric pH

The following subsections deal with the release results of the beads prepared under different synthesis conditions (Tables 3) at gastric pH. Figures 7 to 11 show the % release time plots. Table 6 shows the retention efficiency (EE%), time to reach equilibrium release value (t_e/min), maximum total release (ΣR)max and maximum % release $(R\%)_{max}$ values, i.e. the entrapment and release results for each bead (Figure 6, example calibration curves). The efficiency of Cefaclor to adhere to the beads decreases in the order ACP (93%) > AC (76%) > ACG (46%) = AGP (46%) > AG (40%) > ACGP (39%). Figure 1 also shows that the highest composite drug interaction is ACP-Cef.

3.4.1 Entrapment Efficiency and Release Kinetics of the Alginate-Carrageenan Spheres

In this section, the effects of various parameters on the entrapment percentage and release kinetics of the alginate-carrageenan (AC) composite beads were investigated, and the results were presented.

3.4.1.1 The AC Spheres with Different Drug Concentrations

The synthesis conditions for the AC spheres containing different concentrations of drugs are shown in Table 3. The change in the release kinetics of the beads containing 50 to 500 ppm Cefaclor is presented in Figure 7, and the results are presented in Table 6 (Section 1).

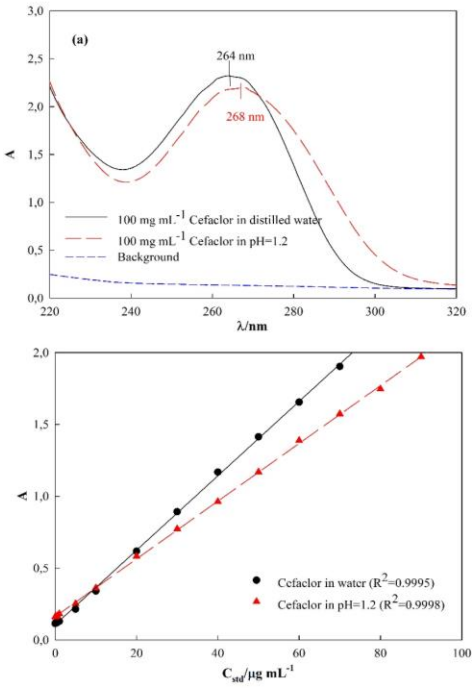

Figure 6. (a) UV absorption spectra of Cefaclor in distilled water and gastric pH, shown with that of the background; **(b)** sample calibration curves.

It was observed that in the samples with different drug concentrations (AC-Cef1-5), the greater the amount of Cefaclor added to the environment, the greater the release. AC-Cef-5 was the sample with the highest drug

concentration and highest release percentage. Thus, it can be concluded that the release percentage is inversely proportional to the retention percentage.

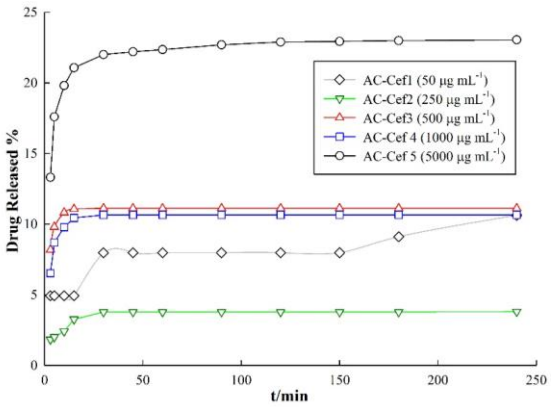

Figure 7. Release profiles of the alginate-carrageenan-Cefaclor (AC-Cef) spheres with different Cefaclor concentrations

Rasool and Fahmy also found that increasing the cefaclor concentration from 5% to 10% (m/V) resulted in better cefaclor retention in chitosan-alginate beads. The burst effect is observed in alginate-containing support materials in the first 30 minutes. The fact that the beads containing chitosan-alginate burst at pH 1.2 within the first 30 minutes. This was attributed to the protonation of the negatively charged carboxyl groups of sodium alginate to form -COOH, thus reducing the degree of crosslinking due to inter-chain electrostatic interactions. In addition, Cefaclor, a small hydrophilic molecule, is highly ionized at this pH; its solubility increases and spreads easily (Rasool and Fahmy 2013). A similar situation is valid for the present study.

3.4.1.2 Release Kinetics of the AC Spheres Containing Different Amounts of Salt

In this section, release experiments were carried out for the AC spheres with different amounts of $CaCl_2$ and KCl in the bead formation medium. The synthesis conditions are shown in Table 3, and the data can be seen in Figure 8a and Table 6 (section 2). The best entrapment between the AC samples with different masses of salt (AC-Cef and AC1-3-Cef) was observed in the AC-Cef composite (2.5% a $CaCl_2$ and 3.3% KCl, salt concentrations = 0.3 mol L^{-1}), while it was observed in the AC3-Cef composite, in which the salt rate was 3%, in the second row. The retention rate increased with cross-linking, as the excess salt in the precipitator medium increased. The AC1-Cef sample, which had the smallest salt mass, had the highest total release percentage. However, when the salt mass was low, the cross-linking rate decreased, and the release became easier. The AC1-Cef and AC2-Cef samples, containing 1% and 2% salt respectively, demonstrated a notable extension in release time, with a sustained increase up to the 240th minute. In a similar vein, the findings of Singh et al.'s study (2021) demonstrated that the quantity of $CaCl_2$ is the pivotal factor in enhancing %EE by augmenting the cross-linking property of Na-Al (Singh et al. 2021). In the studies by Liu et al, the retention of the calcein drug in the alginate-PLGA microparticles was also increased due to the high affinity between the calcium ions used for gelation of the alginate core and calcein (Liu et al. 2016).

Table 6. Entrapment and release results of the composite microbeads

Sample Codes	EE/%	t_e/min	$(\Sigma R)_{max}$/mg cef g^{-1} dry bead	$(R)_{max}$/%
1. Alginate-Carrageenan-Cefaclor beads with different concentration of Cefaclor (μg mL^{-1})				
AC-Cef 1	75.9	240	0.2	10.6
AC-Cef 2	61.5	30	0.3	3.8
AC-Cef 3	56.4	30	1.2	11.1
AC-Cef 4	25.4	30	1.3	10.6
AC-Cef 5	40.5	300	21.7	23.1
2. Alginate-Carrageenan-Cefaclor beads with different amounts (%) of salt (KCl, $CaCl_2$) in the synthesis media				
AC-Cef	61.5	30	0.3	3.8
AC1-Cef	33.9	240	1.3	33.0
AC2-Cef	43.0	240	1.0	23.2
AC3-Cef	45.7	30	0.4	9.0
3. Alginate-Cefaclor and Alginate-Carrageenan-Cefaclor beads with different amounts (mg) of alginate and carrageenan				
A-Cef	36.1	180	2.2	76.4
AC1-Cef	33.9	240	1.3	33.0
AC4-Cef	38.4	180	1.5	50.4
4. Alginate-Carrageenan-PLGA-Cefaclor beads with different PLGA mass (mg)				
AC-Cef	61.5	30	0.3	3.8
ACP10-Cef	48.4	90	1.6	49.8
ACP11-Cef	45.5	90	1.8	77.3
ACP12-Cef	44.8	45	0.9	38.5
5. Alginate-Carrageenan-PLGA-Cefaclor beads with different amounts (%) of PVA in the synthesis media				
ACP10-Cef	35.4	240	1.8	65.5
ACP13-Cef	17.0	60	1.0	69.2
ACP14-Cef	35.7	240	1.3	36.4
6. Alginate-Carrageenan-PLGA-Cefaclor beads with different amounts (mg) of alginate and carrageenan				
AP-Cef	65.5	180	1.4	39.4
ACP9-Cef	93.1	240	1.3	24.1
7. Alginate-Gelatine-Cefaclor beads with different amounts (mg) of alginate and gelatin				
A-Cef	36.1	180	2.2	76.4
AG-Cef	39.6	90	0.4	12.2
AG1-Cef	40.1	180	1.75	60.8
8. Alginate-Gelatine-PLGA-Cefaclor beads with different amounts (mg) of alginate and gelatin				
AP-Cef	65.5	180	1.4	39.4
AGP-Cef	36.1	45	0.8	29.7
AGP1-Cef	45.8	180	1.3	51.9
9. Alginate-Carrageenan-Gelatine-PLGA-Cef beads with different amounts (mg) of alginate, carrageenan and gelatin				
ACG-Cef	45.8	120	0.7	20.0
ACG1-Cef	36.1	120	2.1	90.0
ACGP-Cef	39.1	180	1.8	74.0

3.4.1.3 Release Kinetics of the Composites with Different A and C Masses

In this section, please refer to Table 6, Section 3, which shows the data calculated for the spheres synthesized with different amounts of alginate and carrageenan (see Table 3). Figure 8b shows the release graphs.

Although the AC1-Cef contains 100 mg of alginate and carrageenan in a 10 mL gel medium, it was used in this composite for comparison since it was prepared under conditions equivalent to 150 mg A and C in a 15 mL gel medium.

The entrapment in the samples with different alginate and carrageenan mass ratios was higher in the bead coded AC4-Cef, where the A:C ratio was 2:1, compared to the AC1-Cef, which contained A-C at a ratio of 1:1, and to the A-Cef, which did not contain carrageenan. The addition of C to the medium increased the retention efficiency due to the sulphate groups. The highest total release percentage was observed in the sample A-Cef, which consisted of only alginate and decreased with the addition of C. Besides, while the other two examples showed a burst in 180 minutes, in the sample coded AC1-Cef, the release time exceeded 240 minutes. A similar situation was observed in an α-amylase release study of alginate-carrageenan spheres. The order of cumulative release percentage at pH = 1.8 was reported to be Alg > Alg:Car (3:1) > Alg:Car (1:1) > Alg:Car (1:3). This was explained by the strong electrostatic interactions between the positively charged protein and the negatively charged sulfo- groups of κ-carrageenan, which reduced the drug release in an acidic environment. The same study also reported that microspheres could not be used as a drug release system in the intestine (Kolesnyk et al. 2015).

This result is also in line with previous report confirming that Alginate concentrations have a significant effect on drug release (Singh et al. 2021)

3.4.2 Entrapment Efficiency and Release Kinetics of the Alginate-Carrageenan-PLGA Composite Spheres

In this section, the effects of various parameters on the entrapment percentage and release kinetics of the tri-component composite spheres containing A, C and P were investigated. The results are presented in Figure 9.

3.4.2.1 The ACP Spheres Containing Different Amounts of PLGA

The entrapment efficiency and release data of the beads containing 50, 100 and 200 mg PLGA, whose synthesis conditions are given in Table 3, are presented in Table 6 (section 4) and Figure 9a.

In the samples synthesized by adding different masses of P to the AC sample medium, it was observed that the addition of P (ACP-Cef, ACP1-Cef, ACP2-Cef) reduced the entrapment of the samples compared to the sample coded AC-Cef, where A-C was taken in equal mass and P was not. Although the total composite mass increased from 0.2 g to 0.25, 0.30 and 0.40 g, the best entrapment of the samples with P was observed in the sample coded ACP-Cef, which contained the least PLGA. This indicates that the drug has no affinity for PLGA in the ACP composites. On the other hand, the entrapment levels of the A-Cef (total mass 0.3 g) and AP-Cef (total mass 0.4 g) samples were 36% and 66%, respectively.

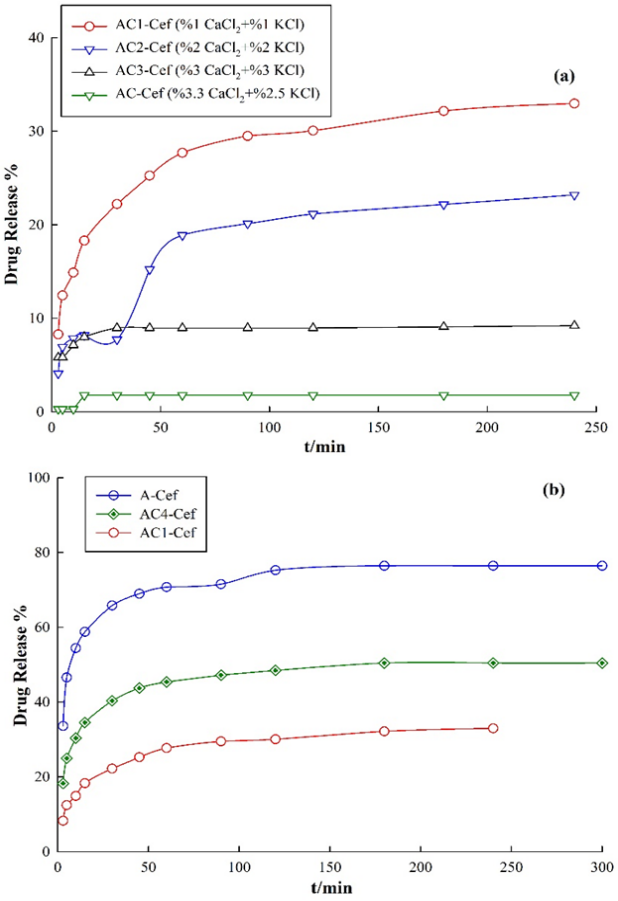

Figure 8. Release plots of **(a)** AC-Cef spheres containing different amounts of salt in the synthesis medium and **(b)** AC-Cef spheres containing different amounts of alginate and carrageenan in the synthesis medium.

Analysis of the composites with different masses of PLGA shows that the sample coded ACP11-Cef, to which PLGA was added at the same mass as A-Cef, gave the best total release percentage, which is also inversely proportional to the entrapment percentage.

In a study investigating the release of calcein from core-shell alginate-poly(lactic-co-glycolic) acid (PLGA) microparticles, alginate-PLGA microparticles were synthesized by double emulsion solvent extraction and

simultaneous ionotropic gelation. While the amount of PLGA was constant in the preparation of PLGA microparticles carrying hydrophilic charges, the particle size and in particular the alginate core size varied. Alginate-PLGA particles with smaller alginate cores showed the slowest drug release (Lio et al. 2016).

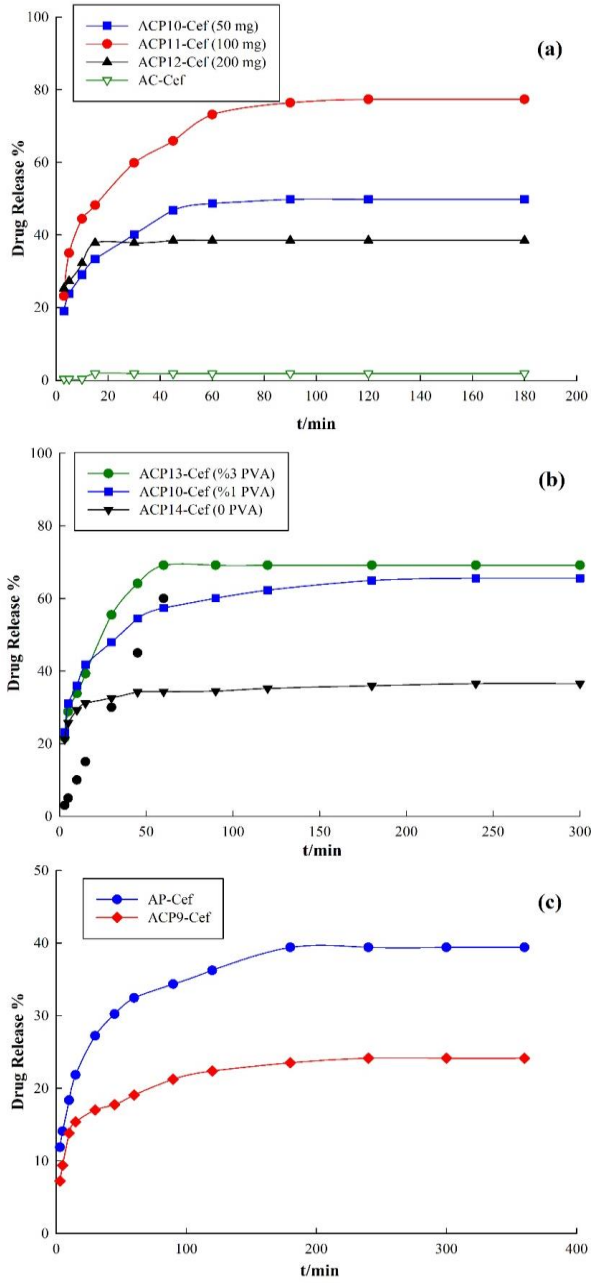

Figure 9. Release plots of **(a)** ACP-Cef composites with different PLGA masses, **(b)** ACP-Cef composites synthesized in different amounts of PVA, and **(c)** AP-Cef and ACP-Cef composites with different masses of A and C.

3.4.2.2 The ACP Composites Synthesized in Media Containing Different Amounts of PVA

In this section, Figure 9b shows the release kinetics graphs drawn for the ACP beads synthesized in the presence of different amounts of PVA in the bead medium (Table 3). In contrast, Table 6-section 5 shows the percentage retention efficiency, the time to reach the maximum release value and the equilibrium release values.

As mentioned above, PVA was added to the synthesis medium to stabilize the PLGA emulsion. The presence of 1% PVA in the medium did not alter the retention efficiency. The percentage release results showed that although the ACP13-Cef synthesized in a medium containing 3% PVA showed the highest release, the sample with 1% PVA encoded ACP10-Cef was more advantageous in terms of delayed release. The high amount of PVA in the medium increased the -OH groups, which reduced cefaclor entrapment and caused bursts in acidic conditions within the first hour. Brough et al. (Brough et al. 2016) also demonstrated that polyvinyl alcohol increased the solubility of itraconazole, a poorly soluble drug.

3.4.2.3 The ACP Composites with Different A and C Masses

The synthesis conditions are given in Table 3 (AP, AP-Cef, ACP, ACP-Cef). The release kinetics graphs drawn for the ACP beads containing different amounts of alginate and carrageenan are shown in Figure 9c and the percentage retention efficiency, the time to reach the maximum release value and the equilibrium release values are shown in Table 6-section 6.

A comparison of the release kinetics of the AP-Cef and ACP9-Cef composites containing different amounts of alginate also shows the contribution of carrageenan to entrapment and release. As shown in Figure 9c and Table 6, the addition of carrageenan to the medium reduced the entrapment efficiency and caused a 15% decrease in release. In addition, it did not contribute significantly to the enhancement of release.

3.4.3. Entrapment Efficiency and Release Kinetics of the Alginate-Gelatine Spheres

In this section, the release kinetics (Figure 10a) of AG spheres containing alginate and gelatin in different masses, whose synthesis conditions are given in Table 3, were studied.

Table 6-section 7 shows that the entrapment percentage did not change significantly, but the release percentage values were quite different for the samples containing different alginate and gelatin (A-Cef, AG-Cef, AG1-Cef). The addition of gelatin to the medium increased the entrapment by only about 4%. In comparison, adding 100 mg of gelatin reduced the release by about 16%, and adding 150 mg reduced the release sixfold. Furthermore, the results for the alginate-gelatin composites were

similar to those for the alginate-carrageenan samples (Figure 8a, Table 6-section 3).

This is due to the strong hydrogen bonds and electrostatic interactions between the alginate and gelatin molecules, as described in the study by Kolesnyk et al. (2015), or between the alginate and carrageenan, as described by Xiao et al. (Xiao et al. 2007).

3.4.4. Entrapment Efficiency and Release Kinetics of the Alginate-Gelatin-PLGA Composites

In this section, the release kinetics were plotted for the spheres synthesized with the AGP content. Figure 10b and Table 6-section 8 show the retention efficiency and release results.

In the samples formed by adding PLGA to the medium with alginate-gelatin, the order of the entrapment percentage was AP-Cef (3:0) > AGP1-Cef (2:1) > AGP-Cef (1:1) according to the alginate: gelatin ratio. This order was AGP1-Cef (2:1) > AP-Cef (3:0) > AGP-Cef (1:1) for the cumulative release percentage.

A general comparison between the samples formed by adding P to A-C and adding P to A-G indicated that the retention efficiency was 93% for the ACP9-Cef synthesized under the same conditions. In comparison, it was 46% for the AGP1-Cef. It is clear that the contribution of C to the composite was higher than that of G, and it depended on the ionic interactions between the $-SO_3^-$ functional groups in the carrageenan and on the positively charged drug in the chloride structure.

3.4.5 Entrapment Efficiency and Release Kinetics of the Alginate-Carrageenan-Gelatin and Alginate-Carrageenan-Gelatin-PLGA Composite Spheres

In this section, the retention efficiency was calculated for the beads synthesized as A-C-G and A-C-G-P. Table 6-9 shows the time to reach the maximum release, total release and release percentage values, and Figures 10c and 10d show the release graphs drawn for the composites, respectively.

The ratio of the components was 1:1:1, the retention efficiency was 46% and the total release was 20% for the triple A-C-G-Cef composites. When the ratio was 4:1:1, the retention efficiency decreased (36%) and the percentage of release increased 4.5 times. This is consistent with previous results indicating that the high alginate beads release a significant amount of cefaclor at gastric pH. The ACGP quadruple composite, prepared in a 1:1:1:1 ratio by adding PLGA to the medium, decreased entrapment and increased release. This can be explained by the interactions between drug-polymer mixtures mentioned above.

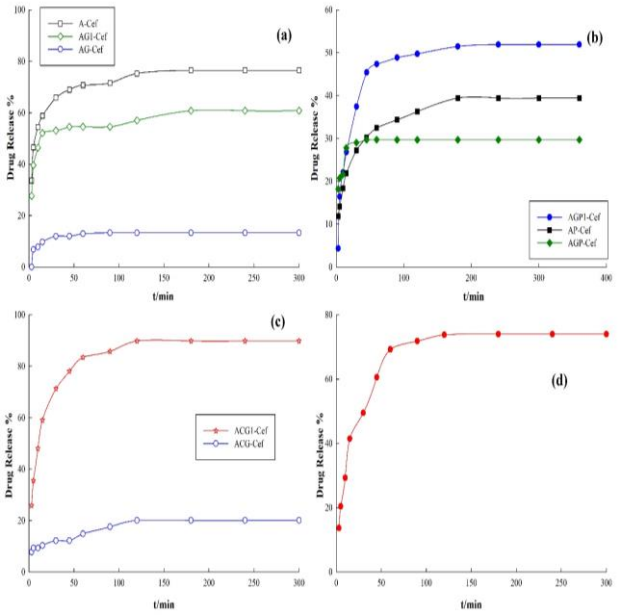

Figure 10. Release profiles of **(a)** AG-Cef composites with different alginate and gelatin masses; **(b)** AGP-Cef composites with different masses of A and G; **(c)** ACG-Cef composites with different masses of alginate, carrageenan, and gelatin; and **(d)** ACGP-Cef composite containing alginate, carrageenan, gelatin, and P.

3.5 Fitness to the Release Kinetics Models and Comparison with the Literature

Considering the total release and total release percentage data, the samples with the highest release values were selected and the suitability of these samples for the following release kinetics models was investigated. The mathematical equations used in the application of the models are presented in section 3.1.

Table 7 shows the R^2 values and release kinetics constants obtained from linearized graphs. The tables indicate that the samples fit with the Korsmeyer-Peppas, first-order release kinetics, and Higuchi release kinetics models, respectively, according to the R^2 values. The fit to the first-order release kinetics observed in porous matrices (i.e., those containing water-soluble drugs), which applies to pharmaceutical dosage forms, is an expected result (Dash et al. 2010).

Especially the n values calculated according to the Korsmeyer-Peppas model show that although it varies according to the composite content, an n value close to 0.5 and below proves that the release kinetics fit the Fick diffusion. For the n values close to 0.5, the water penetration rate was lower than the degradation rate of polymer chains. For the n values below 0.5, the diffusion rate was much lower than the expansion rate of the polymer chains. A recent study developed a sustained release system for cefaclor using nanocomposite clay

(montmorillonite) and polymer (Na-alginate) based microbeads. The study concluded that drug release followed a non-fickian diffusion pattern coupled with matrix release, as indicated by the Korsemeyer-Peppas (n) value of 0.72. As shown in Table 8, the coefficients and release kinetics results obtained from the fitness of the composite beads used in this study to the models above were compared with the other carriers used in the release studies of Cefaclor in the literature. The final section of the table provides the smallest and largest entrapment efficiency (range), maximum release percentage interval, and time interval required to reach this release value for these composites synthesized under different conditions.

A comparison with other carriers can only be made with the study of Chilukala et al. 2016. Floating spheres containing Hydroxyl propyl methylcellulose (HPMC K4M) and ethyl cellulose did not show burst at simulated gastric pH, and the release continued to increase for up to 12 hours. According to the present study, the spheres can only remain in the gastric pH during digestion. The release of Cefaclor from these spheres occurs during digestion, followed by dissipation in the intestinal pH, resulting in the complete release of the drug into the environment. It is noteworthy that no bursts were observed in the initial 30 minutes in a significant number of spheres, which is a notable benefit in release studies.

Table 7. R^2 and release rate constants calculated for various release kinetics models of the samples with the following codes

Sample	Korsmeyer-Peppas			Zero Order		First Order		Higuchi	
Codes	R^2	N	k/ min^{-1}	R^2	k_0/ min^{-1}	R^2	k_1/ min^{-1}	R^2	k_H/ min^{-1}
A-Cef	0.991	0.130	0.271	0.861	0.007	0.982	0.018	0.971	0.160
AC-Cef5	0.907	0.271	0.327	0.832	0.786	0.971	0.052	0.882	0.151
AC1-Cef	0.984	0.438	0.787	0.998	0.009	0.987	0.011	0.958	0.134
ACG1-Cef	0.988	0.388	0.686	0.916	0.031	0.991	0.020	0.996	0.174
AP-Cef	0.991	0.427	0.779	0.942	0.014	0.991	0.017	0.889	0.183
ACP10-Cef	0.995	0.324	0.676	0.909	0.012	0.995	0.011	0.999	0.118
ACP11-Cef	0.985	0.365	0.553	0.905	0.019	0.990	0.023	0.967	0.112
ACP12-Cef	0.991	0.255	0.557	0.885	0.018	0.992	0.011	0.925	0.148
ACGP-Cef	0.999	0.489	0.897	-	-	0.996	0.015	0.999	0.175

Table 8. Comparison of the compounds used in the present study with the release kinetics of some carriers used in Cefaclor release in the literature

Carrier	EE%	Release Time	R%	pH	t/°C	Model	Refer.
Microspheres containing polyvinyl pyrrolidone / ethyl cellulose	38-98	> 1 h Up to 14 h	38-100	Water	37	Higuchi (best fit R^2=0.995, k=64.5	Chow et al. 1998
Microspheres containing alginate and formed by adding chitosan, HMPC, and lactose to alginate	-	3 to 10 h (depending on pH and composite content)	80- 100	1.2 buffer solution, 7.4 buffer solution	37	Zero release kinetics	Bak et al. 2002
Microspheres containing mucin and gelatin	19.5-53.5	First release 10min Up to 4-6 h	60- 100	7.4	37.5	-	Ofokansi et al. 2009
Microspheres coated with chitosan, alginate, ethylcellulose, and cellulose acetate	15	≤ 12 h	60-80	1.2 HCl 4.6 acetate buffer, 6.8 phosphate buffer	37	Korsmeyer-Peppas (in accordance with Fick's law)	Rasool and Fahmy, 2013
Floating spheres containing hydroxypropyl methylcellulose and ethylcellulose	78.8±2.5	12 h	93.6 ± 1.25	1.2 HCl	37±0.5	-	Chilukala et al. 2016
Clay (montmorillonite) and polymer (Na-alginate) based nanocomposite microbeads.	60-90	12 h	50-90 (in 8 h)	pH 1.2 HCl for 2 h and then in 6.8 pH phosphate buffer	37 ± 0.5	Korsmeyer-Peppas	Singh et al. 2021
Alginate (A) Alginate-carrageenan (AC) Alginate-gelatin (AG) Alginate-carrageenan-gelatin (ACG) Alginate-PLGA (AP) Alginate-carrageenan-PLGA (ACP) Alginate-gelatin-PLGA (AGP) Alginate-carrageenan-gelatin-PLGA (ACGP)	36 25-76 40 36-46 66 17-93 36-46 39	180 min 30-300 min 90-180 min 120-180 min. 180 min. 45-240 min. 45-180 min. 180 min	76 4-50 12-61 20-90 39 24-77 30-52 74	1.2 HCl	36	Korsmeyer-Peppas Model, First Order Release, Higuchi Model	This study

4. Conclusion

In the present study, novel composite structures were synthesized by incorporating carrageenan, gelatin, and PLGA into and/or on the surface of the egg-box cage structures in the presence of alginate $CaCl_2$. The structural characterization of these composite spheres was presented in a separate study. In this study, the focus was on comparing the FTIR spectra of medicated and drug-free composite beads for characterization purposes, and it was concluded that the composite with the highest Cef was ACP. The study also investigated the swelling kinetics of pH-sensitive composites and the release of the Cefaclor antibiotic agent at gastric pH.

An examination was conducted to assess the stability of the composites under various pH conditions, specifically at gastric (pH = 1.2, HCl) and intestinal (pH = 7.4, phosphate buffer) levels. The mass loss at the conclusion of the 14th day at acidic pH was observed to range from 9% to 76%, while the structures were found to be fully dispersed by the third day in the buffer medium.

In these swelling experiments, no significant contribution of PLGA to AC to swelling was observed. The change in the swelling amount (percentage swelling) of the ACP beads in the swelling medium follows the trend: water > HCl (pH 1.2) > PB (pH 7.4) > NaOH (pH 10.0). The highest swelling value (641%) was observed for the ACGP-coded bead in water. The swelling values of the A and AP beads in water were higher (981% and 747%, respectively).

The capture efficiency of the Cefaclor loaded by synthesis into spheres containing only alginate (A) was 36%. This efficiency increased to 76% when carrageenan was added to the medium, to 40% when gelatin was added, and to 46% for the triple composites. A similar trend was observed in the binary composites containing only alginate and PLGA (P), with a capture efficiency of 66%, which increased to 93% when carrageenan was added to the medium (ACP).

The time taken to reach the maximum release balance was 3 hours in the spheres containing only A, while it was 3 hours in the AG and ACG and up to 5 hours in the AC spheres. The efficiency was found to be 46% when gelatin was added (AGP) and 39% in the quaternary composite. While the time taken to reach the maximum release balance was 3 hours in the AP-only, AGP, and ACGP spheres, it was 4 hours in the ACP spheres.

Cefaclor is currently known to be sold in extended-release tablets. In this study, the composites obtained were not compared with these tablets; Cefaclor was used only as a sample antibiotic. The focus of the study is to prepare triple and quadruple composite beads containing alginate, investigate their swelling characteristics, and check their usability in an application area. The release of Cefaclor at acidic pH was significantly reduced, and the burst effect of the drug was reduced compared to some materials in the literature and the alginate/Ca2+ microspheres. Therefore, it can be concluded that the microspheres synthesized are efficient for release at the stomach pH, which remains effective for an antibiotic such as Cefaclor.

The most significant limitation of the study is that it could not be conducted in an artificial intestinal environment. In future studies, corrections should be made to increase the durability of the materials in the pH = 7.4 environment. In addition, the materials should be studied in an in vitro environment.

Declaration of Ethical Standards

This study is derived from the master thesis (thesis number: 562048) titled Cefaclor Release with Biodegradable Polymer/Polysaccharide Composites completed by Buse SEMERCİ ARIKAN on 09/07/2019 under the supervision of Assoc. Prof. Dr. Demet BAYBAŞ.

The authors declare that they comply with all ethical standards.

Credit Authorhip Contribution Statement

Author: Conceptualization, investigation, methodology and software, visualization and writing – original draft, supervision and writing – review and editing.

Data availability Statement:

The raw/processed data required to reproduce these findings cannot be shared due to technical or time limitations.

Competing Interests:

Authors declare not to have financial or non-financial interests directly or indirectly related to the work submitted for publication.

Acknowledgment:

We would like to thank Sivas Cumhuriyet University CÜBAP research fund for their support for this study. In addition, the authors would like to thank Centrient Pharmaceuticals (DSM Sinochem Pharmaceuticals, Rotterdam, Netherlands) for providing Cefaclor.

5. References

Arsalan, A., Ahmad, I., Ali, S., A. 2017. in. Berthardt, L,V, (ed). Advances in Medicine and Biolog: Nova Science Publishers Inc., 123**.** pp 1-52.

Bak, S., Lee, J.Y., Song, H., Hwang, J.H. and Lee, S.J. (2002). Controlled release and stabilization of Cefaclor from alginate-based matrices for oral delivery design. *Journal of Pharmaceutical Investigation,* **32**, 327-330.

Baybaş, D., Serdaroğlu, G. and Semerci, B. 2021. The composite microbeads of alginate, carrageenan, gelatin, and poly (lactic-co-glycolic acid): Synthesis, characterization and Density Functional Theory calculations. *International Journal of Biological Macromolecules*, **181,** 322-338.

https://doi.org/10.1016/j.ijbiomac.2021.03.128

Brough, C., Miller, D.A., Keen, J.M., Kucera, S.A. and Lubda, D, 2016. Use of polyvinyl alcohol as a solubility-enhancing polymer for poorly water soluble drug delivery (Part 1). *An Official Journal of the American Association of Pharmaceutical Scientists,* **17(1)**, 167-179.
https://doi.org/10.1208/s12249-015-0458y

Cavallaro, G., Fresta, M., Giammona, G., Puglisi, G. and Villari, A. 1994. Entrapment of β-lactams antibiotics in polyethylcyanoacrylate nanoparticles: Studies on the possible in vivo application of this colloidal delivery system. *International Journal of Pharmaceutics*, ***111*(1)**, 31-41.
https://doi.org/10.1016/0378-5173(94)90399-9

Chilukala,S., Bontha, V.K., Pragada, R.R., 2016. In vitro and in vivo characterization of cefaclor loaded floating microspheres. *Indo American Journal of Pharmaceutical Research* **6(04)**, 5277.

Chow, A.H., Ho, S.S., Tong, H.H. and Ma, H.H. 1998. Parameters affecting in-liquid drying microencapsulation and release rate of cefaclor. *International journal of pharmaceutics*, ***172*(1-2)**, 113-125.
https://doi.org/10.1016/S0378-5173(98)00199-9

Chuang, J.J., Huang, Y.Y., Lo, S.H., Hsu, T.F., Huang, W.Y., Huang, S.L. and Lin, Y.S. 2017. Effects of pH on the shape of alginate particles and its release behavior. *International Journal of Polymer Science*, ***2017*(1)**, 3902704.
https://doi.org/10.1155/2017/3902704

Dash, S., Murthy, P.N., Nath, L. and Chowdhury, P. 2010. Kinetic modeling on drug release from controlled drug delivery systems. *Acta Poloniae Pharmaceutica, **67*(3)**, 217-223.

Davidovich-Pinhas, M. and Bianco-Peled, H. 2010. A quantitative analysis of alginate swelling. *Carbohydrate Polymers*, ***79*(4),** 1020-1027.
https://doi.org/10.1016/j.carbpol.2009.10.036

Faizan, M., Javed, M., Fatima, M., Bahadur, A., Iqbal, S., Mahmood, S. and Ibrahium, H.A. 2024. Incorporation of silane-modified halloysite into hydrogels for Cefaclor drug Release: Potential for wound healing application. *Inorganic Chemistry Communications*, ***163*,** 112351.
https://doi.org/10.1016/j.inoche.2024.112351

Jamroży, M., Kudłacik-Kramarczyk, S., Drabczyk, A., and Krzan, M., 2024. Advanced Drug Carriers: A Review of Selected Protein, Polysaccharide, and Lipid Drug Delivery Platforms. *International Journal of Molecular Sciences, **25 (2)**,* 786.
https://doi.org/10.3390/ijms25020786

Karadağ, E., Ödemiş, H., Kundakçi, S. and Üzüm, Ö.B. 2016. Swelling characterization of acrylamide/zinc acrylate/xanthan gum/sepiolite hybrid hydrogels and Its application in sorption of janus green B from aqueous solutions. *Advances in Polymer Technology*, ***35*(3)**, 248-259.
https://doi.org/10.1002/adv.21547

Kasai, R.D., Radhika, D., Archana, S., Shanavaz, H., Koutavarapu, R., Lee, D.Y. and Shim, J. 2023. A review on hydrogels classification and recent developments in biomedical applications. *International Journal of Polymeric Materials and Polymeric Biomaterials*, ***72*(13)**, 1059-1069.
https://doi.org/10.1080/00914037.2022.2075872

Kolesnyk, I., Konovalova, V. and Burba, N.A. 2015. Alginate/κ-carrageenan microspheres and their applicatıon for protein drugs controlled release. *Chemistry and Chemical Technol*ogy, **9(4)**, 485.

Lin, C.C. and Metters, A.T. 2006. Hydrogels in controlled release formulations: network design and mathematical modeling. *Advanced drug delivery reviews*, **58**(12-13), 1379-1408.
https://doi.org/10.1016/j.addr.2006.09.004

Likhariya, M., Trivedi, D., Bhadoria, J., and Modi, A., 2021. Formulation and evaluation of cefaclor extended-release tablet. *Journal of Drug Delivery and Therapeutics,* **11(6-S),** 33-36.
https://doi.org/10.22270/jddt.v11i6-S.5193

Lio, D., Yeo, D. and Xu, C. 2016. Control of alginate core size in alginate-poly (Lactic-Co-Glycolic) acid microparticles. *Nanoscale Research Letters*, **11**, 1-6.
https://doi.org/10.1186/s11671-015-1222-7

Lorenz, L.J., Cefaclor. in: Florey, K. (ed.) 1980. Analytical profiles of drug substances, Academic Press, New York, vol. 9, 107–123.
https://doi.org/10.1016/S0099-5428(08)60138-0

Mishra, M., (Ed.) 2015. Handbook of encapsulation and controlled release. CRC press. New York.

Ofokansi, K.C,. Okorie, O. and Adikwu, M.U. 2009. Biodegradable microspheres based on gelatin–porcine mucin admixtures: In vitro and in vivo delivery studies*. Biological and Pharmaceutical Bulletin*, ***32*(10)**, 1754-1759.
https://doi.org/10.1248/bpb.32.1754

Öztürk, A.A. and Aygül, A. 2020. Design of cefaclor monohydrate containing nanoparticles with extended antibacterial effect by nano-spray dryer: A nanoenglobing study. *Journal of Research in Pharmacy, **24*(1)**, 100-111.
https://doi.org/10.35333/jrp.2020.115

Popa, E.G., Gomes, M.E. and Reis, R.L. 2011. Cell delivery systems using alginate–carrageenan hydrogel beads and fibers for regenerative medicine applications. *Biomacromolecules*, ***12*(11)**, 3952-3961.
https://doi.org/10.1021/bm200965x

Rasool, B.K.A. and Fahmy, S. 2013. Development of coated beads for oral controlled delivery of cefaclor: In vitro evaluation. *Acta Pharmaceutica*, ***63*(1)**, 31-44.
https://doi.org/10.2478/acph-2013-0003

Schott, H. 1992. Kinetics of swelling of polymers and their gels. *Journal of Pharmaceutical Sciences*, **81**, 5, 467-470.

Semerci, B. 2019. Biyobozunur Polimer/Polisakkarit Kompozitleri İle Sefaklor Salımı, Yüksek Lisans Tezi, Sivas Cumhuriyet Üniversitesi Fen Bilimleri Enstitüsü, Sivas, 127.

Singh, S., Raut, S. Y., Kohli, K., & Kumar, S. 2022. Design and development of montmorillonite-sodium alginate microbeads for oral sustained delivery of cefaclor. *Journal of Medical Pharmaceutical and Allied Science*, 11 (3), 2634, 4986-4994. https://doi.org/10.55522/jmpas.V11I3.2634

Sun, S.B., Liu, P., Shao, F.M. and Miao, Q.L. 2015. Formulation and evaluation of PLGA nanoparticles loaded capecitabine for prostate cancer. *International journal of clinical and experimental medicine*, ***8*(10)**, 19670.

Torres, L.G., Velasquez, A. and Brito-Arias, M.A. 2011. Ca-alginate spheres behavior in presence of some solvents and water-solvent mixtures. *Advances in Bioscience and Biotechnology*, ***2***, 8-12 https://doi.org/10.4236/abb.2011.210028-12

Xiao, C., Liu, H., Lu, Y. and Zhang, L.J*,* 2007. Blend films from sodium alginate and gelatin solutions. *Journal of Macromolecular Science, Part A: Pure and Applied Chemistry* A, **38(3)**, 317-328.